Silicate melt inclusions from a mildly peralkaline granite in the Oslo paleorift, Norway

T. H. HANSTEEN

Mineralogical-Geological Museum, Sars Gate 1, N-0562 Oslo 5, Norway*

AND

W. J. LUSTENHOUWER

Netherlands Organization for Scientific Research (NWO), the Free University, N-1007 MC Amsterdam, The Netherlands

Abstract

The mildy peralkaline Eikeren–Skrim granite belongs to the Permian magmatic province of the Oslo rift, south-east Norway. Euhedral quartz crystals from the abundant miarolitic cavities contain primary inclusions of partly crytallized silicate melts and coexisting primary, aqueous fluid inclusions. Microthermometric measurements give maximum estimates for the granite solidus of 685–705 °C. Quenched silicate melt inclusions are not peralkaline, have normative Or/Ab weight ratios of 1.15–1.44 (compared to 0.49–0.80 in whole-rock samples) and F and Cl contents of 0.1 and 0.21–0.65 wt.%, respectively. Coexisting magmatic fluid inclusions are highly enriched in Na, Cl, S and to some extent K. These chemical characteristics are the results of late-magmatic melt–mineral–fluid interaction in the miarolitic cavities.

KEYWORDS: silicate melt inclusions, granite, peralkaline, Oslo rift, Norway.

Introduction

A considerable amount of experimental data exists on solidus and liquidus temperatures of water and halogen-bearing granitic systems (e.g. Tuttle and Bowen, 1958; Bailey, 1977; Manning, 1981). The results show that addition of volatiles to the dry systems decreases liquidus and solidus temperatures, and also changes the compositions of minimum melts. There are, however, potential problems with transferring experimental results to complex natural rock systems. (1) Whole-rock samples do not represent the bulk chemical system because volatiles have exsolved and escaped during the late-stage evolution. (2) Most whole-rock samples contain more than one generation of magmatic minerals. It may thus be difficult to assess the composition of the late-magmatic residual liquids, which in turn is crucial for prediction of solidus temperatures (e.g. Bailey, 1977).

The problems of finding the composition and melting behaviour of late magmatic residual liquids can be overcome by studying samples of silicate melts trapped as inclusions in late-magmatic quartz crystals from miarolitic cavities. Provided that the inclusions behaved as closed systems since the time of trapping, they are unbiased random samples of the late-magmatic liquids. In this paper, microthermometric measurements and microprobe analyses of late-magmatic silicate melt inclusions provide complementary date on late-stage processes in the midly peralkaline Eikeren-Skrim granite complex ('ekerite' in Brøgger's (1906) terminology) (ESG; Fig. 1).

Geology and petrography

The Oslo region alkaline province comprises Permo-Carboniferous lavas and Permian monzonitic to syenitic and grantic intrusions. (Brøgger, 1890, 1906; Ramberg and Larsen, 1978). Igneous activity in the rift covers the time span 300–240 Ma (Sundvoll, 1978; Rasmussen *et al.*, 1988; Neumann *et al.*, 1988). Subvolcanic rocks can be grouped as (*a*) older and younger biotite granites, (*b*) intermediate saturated to understurated rocks (mainly augite monzonite–augite syenite and

* Present address: Nordic Volcanological Institute, University of Iceland, Geoscience Building, 101 Reykjavik, Iceland.

Mineralogical Magazine, June 1990, Vol. 54, pp. 195–205
© *Copyright the Mineralogical Society*

nepheline syenite), and (*c*) alkaline to mildly peralkaline oversaturated rocks comprising alkali syenites and alkali granites (nordmarkite and ekerite, respectively) (Brøgger, 1906; Barth, 1945; Sæther, 1962; Nystuen, 1975; Neumann, 1976, 1978, 1980; Gaut, 1981; Rasmussen *et al.*, 1988).

Dietrich *et al.* (1965) suggested that late-magmatic volatile transfer processes could explain some anomaluosly low but quite variable trace element concentrations peculiar to ekerite. This hypothesis was supported by Raade (1978), and partially by Neumann (1976) and Neumann *et al.* (1977). Isotopic and trace element studies suggest that the ekerite magmas were subject to certain late-stage element-transfer processes in addition to closed-system fractionation (Heier and Compston, 1969; Raade, 1978; Rasmussen *et al.*, 1988). Rasmussen *et al.* (1988) and Neumann *et al.* (1989) have shown that late-stage processes involving fluids were indeed important in the genesis of ekerite trace element characteristics.

The Eikeren–Skrim granite complex (Fig. 1) consists mainly of intermediate to coarse grained (grain size 5–15 mm), hypidiomorphic to allotriomorphic granular rocks with quartz contents of 15–30%. The contents of alkali feldspar phenocrysts are highly variable, and the rock is locally quartz-porphyritic (Hansteen, 1988). The feldspar (60–80%) is mesoperthitic, and covered by rims of nearly pure albite. The rocks are characterized by alkali amphibole which range in composition from manganoan richterite to manganoan arfvedsonite – manganoan magnesio-arfvedsonite (Neumann, 1976; Neumann *et al.*, 1989). Aegirine is usually present. Magnetite, ilmenite (both Mn-rich; Neumann, 1974) and apatite constitute minor phases. Accessory minerals are zircon, ±sphene, ±pyrite, ±rutile, ±fluorite, ±biotite, ±astrophyllite, ±elpidite. The crystallization sequence can be summarized as follows: (1) *Pl*agioclase + *mag*netite ± al*k*ali *f*eld*s*par ± *amph*ibole ± *ilm*enite ± *zir*con ± *ap*atite, (2) amp + kfs + mag ± qtz ± cpx ± ilm ± zir ± ap, (3) kfs + mag + ilm + qtz + cpx + zir + ap ± remaining accessory minerals. In rocks with high pyroxene contents, amph + cpx co-precipitation covers a larger crystallization interval than just mentioned.

Miarolitic cavities are common, and range in sizes from about 1 mm (interstices between mineral grains) to as much as 50 cm (mineral-lined cavities). The larger miaroles are surrounded by transition zones consisting of quartz-perthite graphic intergrowths, which may be intermixed with giant textured quartz and perthite (Hansteen, 1988; Hansteen and Burke, 1989). Several rare minerals have been described from the miarolitic cavities and in the rock proper (Dietrich *et al.*, 1965; Raade, 1972; Neumann *et al.*, 1989).

The two samples chosen for this study (TH88Q1 and TH63/64Q2) are euhedral, slightly smoky quartz crystals which grew directly on quartz–alkali-feldspar graphic zones surrounding the miarolitic cavities (Hansteen and Burke, 1989). Each sample contains several early primary and/or pseudosecondary (Roedder, 1984) silicate melt inclusions, each of which contains mineral grains, partially devitrified glass and a vapour bubble (Fig. 2). The mineral grains constitute at least 60% of the inclusion volume, and are predominantly colourless grains which were tentatively identified as alkali feldspar, but lesser amounts of dark minerals also occur (Hansteen and Burke, 1989). Due to the irregular inclusion outlines, estimates of the relative proportions of glass and vapour are somewhat uncertain, but they probably represent 5–15% and 10–20%, respectively, of the total volume. Inclusion sizes are 15 to 60 μm. Silicate melt inclusions in several samples from the ESG coexist with both primary, high salinity (the inclusions contain daughter minerals of halides ± sulphates at room temperature) and primary vapour-rich, low-salinity aqueous fluid inclusions (Hansteen, 1988; Hansteen and Burke, 1989). This indicates that at least locally, the magmatic fluid were boiling. The quartz crystals additionally contain various trapped mineral grains, e.g. perthite, alkali pyriboles and zircon (identified by electron microprobe).

Methods

Electron microprobe. Electron microprobe analyses were performed on quenched silicate melt inclusions in miarolitic quartz. Analyses were performed on a Cambridge Microscan 9 at the Free University in Amsterdam. Analysed minerals were used as standards. ZAF-corrections were performed on-line using a computer program. Analytical conditions for all elements except fluorine were: raster mode, accelerating voltage 20 kV, sample current 25 nA and counting time 10 seconds. Analytical conditions for fluorine were as above, except for sample current 40 nA and counting time 49 seconds.

Microthermometry. Heating measurements were performed at the Mineralogical-Geological Museum in Oslo using a Linkam TH1500 heating stage in combination with a Linkam TMS90 programmable controller unit and a PU1500 power unit. The following compounds were used to cali-

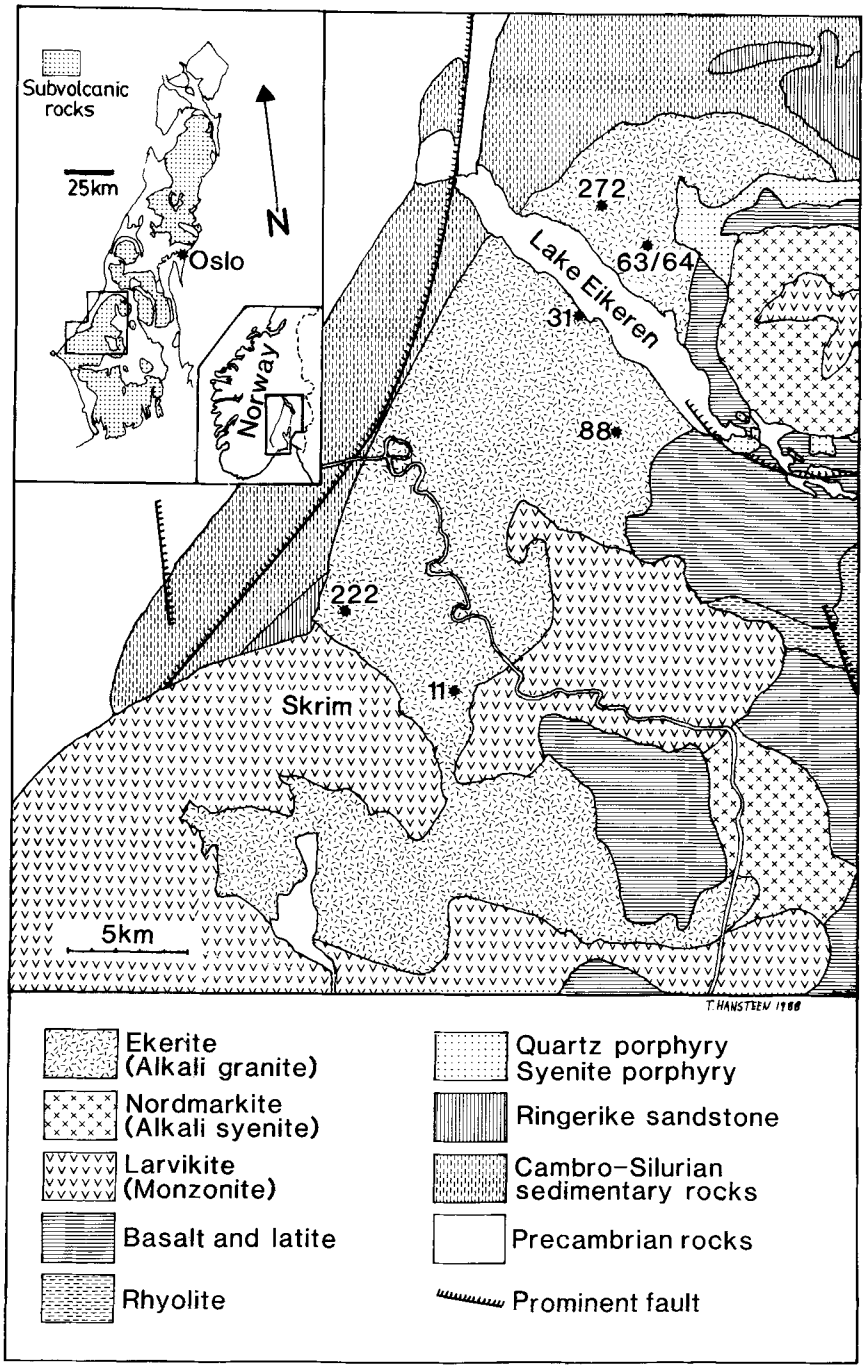

FIG. 1. The Eikeren–Skrim granite complex and its immediate surroundings. Numbers correspond to sample localities. Insert: Schematic outline of the Oslo paleorift, showing the areal extent of subvolcanic rocks. Map after Ramberg (1976), Brøgger and Schetelig (1926), Raade (1973 and unpublished), Andersen (1981) and Hansteen (1988).

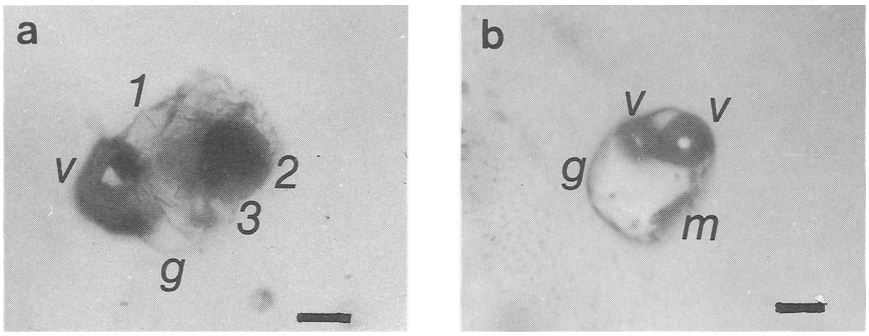

FIG. 2. Silicate melt inclusions from sample 88Q1. Scale bars are 20 m. (*a*) Inclusion IA (see text) prior to heating. V = vapour; G = glass; 1, 2 and 3 denote different mineral grains. (*b*) Quenched inclusion containing 2 vapour bubbles (V), glass (G), a long-prismatic mineral (M) and 3 or 4 small, dark mineral grains.

brate the TH1500 stage (melting points in parenthesis from Weast, 1984): potassium dichromate (398 °C), potassium chloride (770 °C), sodium chloride (801 °C), silver (962 °C) and gold (1064 °C). All substances were at least 99.9% pure (by weight). After several calibration runs, conservative precision estimates of ±15 °C at $T < 700$ °C and ±20 °C at $T > 700$ °C were assigned to all measurements.

Stepwise heating followed by several minutes at constant temperature was utilized in order to approach equilibrium conditions slowly, and thereby minimize overestimation of reaction temperatures. As soon as any visible changes occurred in the inclusions, heating was stopped and the temperature held constant until no further changes occurred. Heating steps close to reaction temperatures were in the order of 5 °C.

Microthermometry

Observations at sub-ambient temperatures. The silicate melt inclusions were cooled to −150 °C, using a Chaixmeca combined heating and cooling stage (Poty *et al.*, 1976) at the Mineralogical-Geological Museum in Oslo. No freezing event was observed in the vapour bubbles or elsewhere in the inclusions. Upon reheating, however, there was a change in refractive indices (RI) between the vapour bubble and surrounding glass between −60 and −50 °C, suggesting the melting of a partially condensed, low density vapour phase containing some CO_2 (CO_2 triple point at −56.6 °C; Weast, 1984). No further phase changes were observed at sub-ambient temperatures.

Observations during heating. The observations described below include about 25 inclusions. Because the silicate melt inclusions in both samples showed similar behaviour, the observations described below are valid for both samples unless otherwise stated.

The first visible changes occurred at *ca.* 550 °C, and were most pronouced in sample 88Q1-4 (Table 1). The glass in the inclusions exhibited a slight decolouration, which is probably best described as a breakdown of the devitrification phases. This was accompanied by a minor change in refractive index (RI) as compared to the host quartz. At 560 °C, the glass became significantly more transparent during 5 minutes. Obvious reaction rims between all major mineral grains and glass appeared at 590 °C. The medium to light brown and irregular reaction rims grew slowly in the course of 5 to 10 minutes, after which they seemingly stabilized at a constant thickness. As some of the vapour bubbles became *slightly* more regular, the reactions seemed to involve some spatial redistribution of the material within the inclusions, possibly due to glass softening. Slow, stepwise heating to 660 °C brought about more reactions, glass decolouration and somewhat more regular bubble outlines (Table 1). At 685 °C, the largest of the colourless mineral grains in two of the inclusions in 88Q1-4 was reduced in size and became slightly rounded. An increase in temperature to between 700 and 705 °C led to similar reactions in several of the remaining inclusions in both samples. After roughly one minute, marked changes occurred in the RIs of the border zones between most mineral grains and glass. This led to a coarse granular appearance of each inclusion as a whole, resembling the first melting in frozen, aqueous inclusions. Heating to 710 °C led to much enhanced reactions in most inclusions. Stringers of yellowish brown melt(?) with RIs dif-

TABLE 1. Summary of important microthermometric data from silicate melt inclusions. See text for discussion of results.

Temperature, °C	Observations
550-560	Glass decolouration.
590	Reaction rims minerals-glass; glass decolouration; slightly more regular bubbles.
660	Enhanced reactions.
685-705	Melting; inclusions turn coarsely granular from internal changes in RI mineral-melt.
705-710	Enhanced melting reactions.
850-910	Strong bubble contraction; complete or nearly complete melting (minus opaques).
900	First homogenization into liquid (melt).

ferent to glass and mineral grains were observed against the inclusion walls and between the mineral-mineral and mineral-glass contacts. Thus, the reaction rims were gradually replaced by melt. The vapour bubbles became markedly more rounded, and their sizes were reduced. In the temperature interval 715 to 750 °C, the overall granularity of the inclusions was much reduced and borders between different domains in the inclusions gradually disappeared. Continued heating of sample 63/64Q2 to 790 °C accomplished further reduction in the sizes of both mineral grains and bubbles.

Heating of sample 63/64Q2 to 910 °C produced the following changes (Table 1): (*a*) reactions (seen as formation of reaction rims) between dark minerals and glass/melt, and (*b*) strong corrosion or complete melting of the colourless minerals. Two or three small opaques and/or dark minerals did not, however, melt completely in any of the inclusions. In three inclusions, the original bubble split into two separate ones in the course of 5 to 10 minutes at 870 °C. After the runs, the samples were brought to room temperature in 10 to 15 minutes.

During heating runs, it became clear that the inclusions did not have equal phase proportions, as seen in the large variations in relative bubble sizes, and also from the variable proportions of dark minerals. Smaller inclusions were observed to have a much higher degree of fill (i.e. a smaller vapour bubble) than the large ones. Each of three inclusions contained one long prismatic, faintly greenish mineral (a pyroxene?), each with a variable size relative to the inclusion.

Sample 88Q1-4 was heated a second time in order to make more measurements. Reactions achieved during the previous run (3 days earlier) were seemingly not reversed to any great extent. The only observed change was a slight colouration of the glass immediately surrounding the dark minerals.

The first changes appeared at 690 °C, when the bubbles (which had changed form upon cooling) became slightly more regular. At 735 °C, brownish 'shadows' developed around the one or two largest dark coloured mineral grains in most of the inclusions: some reaction (rim darkening) was also observed around the largest colourless mineral grains in the biggest inclusion.

The sizes of the light coloured minerals had decreased significantly at 810 °C. The sizes of the vapour bubbles in the smallest inclusions were drastically reduced at 850 °C. Complete melting (excluding opaques) occurred in the range 850 to 900 °C in some of the inclusions (Table 1). Two of the smallest inclusions, one with a large, long prismatic mineral, a small, dark grain and a small opaque, and the other containing the opaque and dark ones only, lost their vapour bubbles by homogenization into melt at 900 to 910 °C. Four other inclusions lost their bubbles at 910, 935, 945 and 955 °C, respectively.

The fast cooling rate used in the experiments (*ca.* 65 °C per minute) effects a quenching of the inclusions. However, all inclusions that had homogenized (by bubble disappearance), restored a bubble upon cooling. The volume of the renucleated bubbles was much smaller as compared to the 'original' ones. This probably reflects the smaller volume occupied by the original glass + 'solids' assemblage as compared to the newly formed glass. An additional factor may be that the original bubbles contained more fluid than the newly formed ones (i.e. more fluid was dissolved in the larger proportion of glass).

TABLE 2. Microprobe analyses of three quenched silicate melt inclusions (IA, IB, and IC respectively) and their CIPW norms. Analyses of perthite lamellae from a coexisting trapped alkali feldspar, as well as four representative whole-rock analyses (Neumann et al., 1989), are shown for comparison. All values are in wt.%. Horizontal bar (-) = not analysed; ND = not detected. FeO/Fe_{TOT} = 0.35 was used in norm calculations for TH11C and TH31.

	IA core	IA rim	IB	IC	Or	Ab	E222	E272	TH11C	TH31
SiO_2	68.57	70.45	69.72	66.21	64.92	68.85	69.51	70.44	76.14	69.73
TiO_2	ND	0.16	0.62	0.06	-	0.04	0.42	0.39	0.19	0.57
Al_2O_3	14.82	14.86	13.57	18.51	18.06	19.13	14.34	13.21	11.18	14.38
Fe_2O_3	ND	ND	ND	ND	ND	ND	1.60	1.70	-	-
FeO	2.51	2.22	2.73	1.65	0.14	0.15	0.72	0.89	3.02	3.90
MnO	0.53	0.51	0.60	0.40	-	ND	0.10	0.12	0.19	0.24
MgO	0.05	0.03	ND	0.03	0.02	ND	0.12	0.13	0.07	0.44
CaO	0.04	0.03	0.07	ND	ND	ND	0.28	0.38	0.01	0.73
Na_2O	3.24	3.04	3.25	3.75	0.49	12.12	5.31	5.21	4.31	5.91
K_2O	6.14	6.29	5.37	8.04	16.60	0.06	5.44	4.54	4.45	4.14
P_2O_5	ND	ND	ND	ND	-	-	0.05	0.06	0.02	0.14
H_2O	ND	ND	ND	ND	-	-	0.22	0.34	0.10	0.16
S	ND	-	0.02	-	-	-	ND	ND	ND	ND
Cl	0.65	0.57	0.21	0.19	-	-	ND	ND	ND	ND
F	0.09	0.09	0.10	0.10	-	-	ND	ND	ND	ND
Total	96.64	98.25	96.26	98.94	100.23	100.35	98.20	97.51	99.70	100.34
	CIPW norms:									
Ap							0.11	0.13	0.04	0.31
Il		0.30	1.16				0.80	0.74	0.37	1.09
Mt	2.10	1.85	2.28				1.43	1.84	0.92	3.32
Or	35.63	36.33	31.13				32.10	26.80	26.58	24.50
Ab	26.93	25.15	26.99				43.42	42.63	33.09	50.10
An	0.19	0.15	0.34							0.48
Di							0.74	1.07		1.97
Hy	0.60	0.43	0.20						0.68	0.25
Ac							1.29	1.25	3.33	
C	5.45	5.87	4.49						0.06	
Q	25.01	27.52	29.35				17.73	22.50	34.58	18.16
Hm							0.17			
Wo							0.10	0.10		
Total	95.90	97.59	95.93				97.89	97.07	99.58	100.18

Microprobe analyses

After quenching from magmatic temperatures, sample 88Q1 was mounted in plastic resin and carefully polished down in order to reach the glass inclusions. Four analyses from three glass inclusions as well as analyses of two lamellae from a perthite grain (marked Or and Ab, respectively) coexisting with the glass inclusions, are given in Table 2. Additionally, four representative whole-rock analyses from the host granite (Neumann *et al.*, 1989) are added for the sake of comparison (Table 2). The glasses have granitic compositions and, except for inclusion IC, they show internally comparable values for all major elements. MgO and CaO contents are consistently low. Fluorine contents are about 0.1 wt.%, while Cl contents range from 0.19 to 0.65 wt.%. Inclusions IB and IA were analysed for S; the S contents are 0.02 wt.% and below the detection limit (*ca.* 0.01 wt.%), respectively. The somewhat low SiO_2 contents of the inclusions as compared to many whole-rock samples may be due to limited crystallization of quartz on the inclusion walls during quenching. Quartz crystallization was not, however, observed during quenching, and the effect is therefore considered to be small. The relatively low sums of the analyses are probably due to dissolved water in the glass. Inclusions IA and IC contain a comparatively large zircon grain (identified by microprobe) which was probably trapped during crystallization of the host quartz.

Compared with the other glass inclusions, inclusion IC has higher alumina and alkali contents and lower silica and iron contents. The silica, alumina and potassium values are in fact very similar to a mesoperthite (cf. Ab and Or analyses in Table 2). It is thus likely that the glass in inclusion IC contains a major component from a trapped perthite grain. Inclusion IC will therefore not be discussed any further.

Discussion and conclusions

Solidus estimates from silicate melt inclusions. The observed inclusions occur in quartz from miarolitic cavities. These inclusions were thus formed at temperatures lower than the liquidi of

the host rocks, and therefore represent residual melts. Compositional relations among mafic silicates in the ekerites suggest that they crystallized under closed-system conditions (Neumann 1976). Provided that the inclusions behaved as closed systems since their trapping, the near-solidus phase relations of these residual melts must therefore closely approach those of the bulk system.

Since the inclusions contain some glass they are not representing a stable sub-solidus phase assemblage. The temperature interval of 685–705 °C observed for the first melting is therefore regarded as a maximum value for the true eutectic melting temperature. Close approach of the observed melting temperatures and a minimum melting is, however, supported by the fact that a temperature increase of only 5 to 10 °C (i.e. from 705 to 710 °C) led to much enhanced reactions. The comparatively rapid heating rates employed may have led to some overstepping of the equilibrium reaction temperatures. This error is, however, considered to be minor (i.e. in the order of 10 °C) based on the reproducibility of the measurements.

The solidus estimate obtained (685 to 705 °C) is in agreement with experimental results in complex granitic systems, if the effect of alkalis, halogens and iron in addition to the major components of 'petrogeny's residua system' (Bowen, 1937) is considered (e.g. Manning, 1981). Experimental liquidus determinations in the systems Ab–Or–Qtz–H_2O (1) and Ab–Or–Qtz–5% $NaFeSi_2O_6$–H_2O (2) at 1 kbar give minima at 730(±5–10) °C (Tuttle and Bowen, 1958; Thompson and MacKenzie, 1967). Analyses of the quenched ESG silicate melt inclusions show F contents of about 0.1 wt.% and Cl contents of 0.19 to 0.65 wt.% (Table 2). Additionally, the presence of F-rich amphibole (Neumann *et al.*, 1989), and sometimes fluorite, as solidus phases in the ESG rocks, indicates that fluorine was fixed at a high activity during the late crystallization of the magma. Experimental and theoretical investigations on various natural and synthetic granite systems, show that F depolymerizes the melt structure, and thereby lowers the solidus temperatures (Manning *et al.*, 1980). Manning (1981) found that the addition of 1 wt.% fluorine to system 1 (above) lowered the minimum from 730 to 690 °C. Assuming that Cl has a similar depolymerising effect on the melt structure as F (e.g. Burnham 1979), the combined effect of F and Cl found in the ESG residual melts would result in roughly similar lowering of the temperature minimum as about 0.5 to 1% of F. Thus, assuming that the effect of F is similar for system 2 (above), the estimated eutectic melting temperatures (685–705 °C) can easily be explained by the moderate halogen contents found in the residual melts (Table 2).

Judging from host-rock mineralogy, the small opaques that do not dissolve at any experimental temperature, could be magnetite. This agrees well with observations by Thompson and Mackenzie (1967) on the experimental system Ab–Or–Qtz–5% $NaFeSi_2O_6$–H_2O in which small amounts of magnetite were found in the glasses quenched from temperatures above the reported liquidi.

Based on compositional relations between mafic minerals in the ESG, Neumann (1976) concluded that the solidus temperature probably was close to 750 °C. Andersen (1984) used mineralogical and chemical considerations to arrive at a solidus temperature of 720–740 °C for the nordmarkitic (i.e. alkali quartz syenitic) part of the nearby Sande cauldron central complex, which is mineralogically similar to the ESG. This estimate is somewhat higher than the present estimate for the granitic counterpart.

Coexistence of magnetite and pyrite in some ESG samples suggest f_{O_2} values above the magnetite–pyrite–pyrrhotite buffer. This is compatible with f_{O_2} estimates for the Sande cauldron nordmarkite (Andersen, 1984).

Water contents in residual melts. Coexistence of primary, aqueous fluid inclusions and silicate melt inclusions in the quartz crystals is strongly suggestive of water over-saturation in the miarolitic cavities. The low sums of the glass analyses (96.26 to 98.25 wt.%; Table 2) indicate water contents of 1.75 to 3.74 wt.% in the melts. This compares well with experimentally determined H_2O saturation values of 2.74 to 2.88 wt.% at 970 bars obtained for rocks with chemical compositions very close to those of the ESG rocks (samples EOR and NOR from Dingwell *et al.*, 1984). Thickness estimates for the overlying Permian lava pile (Oftedahl, 1978) as well as depths of boiling estimated from fluid-inclusion data (Hansteen, 1988) suggest a burial depth of 1.5 to 3 km for the ESG, corresponding to 0.5 to 1 kbar lithostatic pressure.

Heterogeneous silicate melt–mineral–fluid entrapment. The relatively high homogenization temperatures (Table 1) and the variable phase proportions in the silicate melt inclusions can be explained by heterogeneous trapping of minerals, silicate melt and low density aqueous fluid (gas phase) (Hansteen, 1988). Low-temperature measurements on melt inclusions show that their bubbles contain small amounts of a CO_2-bearing fluid phase, and thus do not merely represent contraction bubbles (e.g. Roedder and Coombs, 1967).

Coexistence of the glass inclusions with aqueous fluid inclusions suggest that the vapour bubbles additionally may contain water, but in amounts too small for microthermometric determinations. The low liquid contents in the melt inclusions is probably due to water consumption in the reactions which led to formation of devitrification-phases. Large variations in bubble sizes among the inclusions can be attributed to heterogeneous trapping of silicate melt and variable amounts of an aqueous gas phase. This can also explain the somewhat variable Cl contents in the silicate melt inclusions (Table 2). No examples of heterogeneous trapping of silicate melt and high salinity fluids have been observed. Hansteen (1988) reported that heterogeneous mineral–melt trapping is common in the ESG. Variable mineral contents in the melt inclusions at super-solidus conditions are thus best explained by random trapping of small mineral grains together with the silicate melts.

Chemical evolution. In Fig. 3, compositions of silicate melt inclusions are compared to whole-rock analyses from the ESG (Neumann *et al.*, 1989) suggesting that these particular silicate melt inclusions have compositions similar to certain whole-rock samples. The values for FeO and Al_2O_3 fall within the compositional trends. The data points for Na_2O, however, fall somewhat below the trend defined by the whole-rock samples. Similarly, the K_2O values fall slightly above the main K_2O-trend. These discrepancies can probably be attributed to complex silicate melt–mineral–liquid–vapour equilibria during the late-magmatic stage. The comparatively low SiO_2 values in the inclusions suggest that they represent residual liquids for the less evolved rocks only. This is compatible with petrographic observations from rocks at locality TH88 (T. Hansteen, unpubl. data).

Hansteen and Burke (1989) found that the most abundant species in the magmatic fluid inclusions are Cl, Na, K and S (as sulphate). Sulphur and chlorine contents estimated from daughter mineral contents in fluid inclusions are 0.4 to 4.8 and 18.0 to 29.1 wt.% respectively (Table 3). The lower range of these values correspond to locality TH88. Microthermometric measurements give salinities of 42–63 wt.% NaCl equivalents (Clynne and Potter, 1977), and K and Na contents of 6.8 and 15.4 wt.%, respectively, for magmatic fluid inclusions from TH88 (Table 3) (Hansteen, 1988). When these data are compared with the analyses in Table 2, it is evident that not only chlorine and alkalis, but also sulphate, were strongly partitioned into the aqueous fluid phases. High chlorine contents in the magmatic system enhances

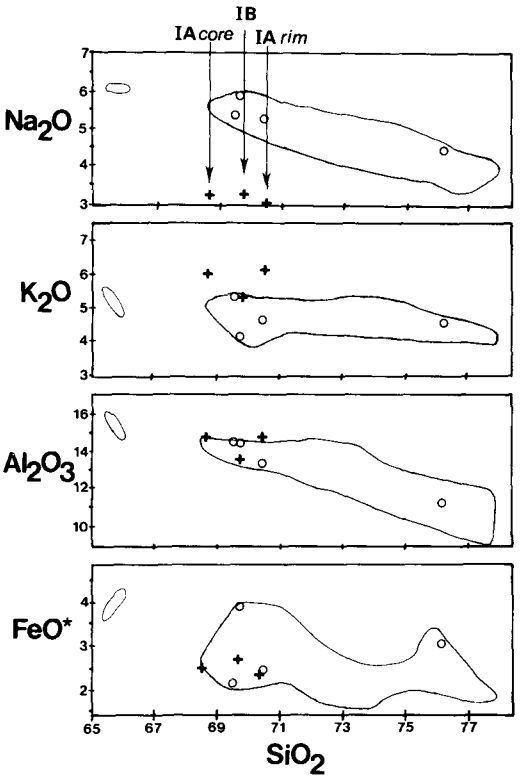

FIG. 3. Comparison between compositions of quenched silicate melt inclusions and whole-rock compositions of ekerites from the ESG (Neumann *et al.*, 1989). Arrows indicate indentities of silicate melt analyses (crosses); selected whole-rock analyses are indicated by circles (cf. Table 2). All values are in wt.% oxides. All iron is given as FeO.

alkali partitioning into the fluid phase (e.g. Holland, 1972). In the ESG, the very high Cl and S contents in the magmatic fluids as compared to the residual melts (Tables 3 and 2, respectively) are probably results of both high fluid/melt partition coefficients and concentration by boiling. The relative influence of the two processes are somewhat uncertain.

In Fig. 4, normative compositions of silicate melt inclusions and representative whole-rock analyses (Table 2) are compared in terms of the system quartz–albite–orthoclase (Qtz–Ab–Or). Fig. 4 additionally shows the liquidus minimum for the system Qtz–Ab–Or with excess water and 1% F at 1 kbar pressure (F) (Manning, 1981) and the similar minimum for the F-free system (M) (Tuttle and Bowen, 1958). The whole-rock analyses cluster around the minimum for the system containing 1% F. This is compatible with moderate halogen contents in the ESG rocks. The sili-

TABLE 3. Estimated major element contents in magmatic fluid inclusions. All values are in wt%. W_S = salinity.

S	0.4- 4.8 *
Cl	18.0-29.1 *
K	6.8 [1,2]
Na	15.4 [1,2]
W_S	42 - 63 wt% NaCl equiv. [3]

*) Estimated from daughter mineral contents (Hansteen and Burke, 1989).
1) Estimated from dissolution temperatures of coexisting halite and sylvite in inclusions (Sterner et al., 1988) (Hansteen, 1988).
2) At locality TH88.
3) Calculated from final halite dissolution temperatures in inclusions (Chou, 1987) (Hansteen, 1988).

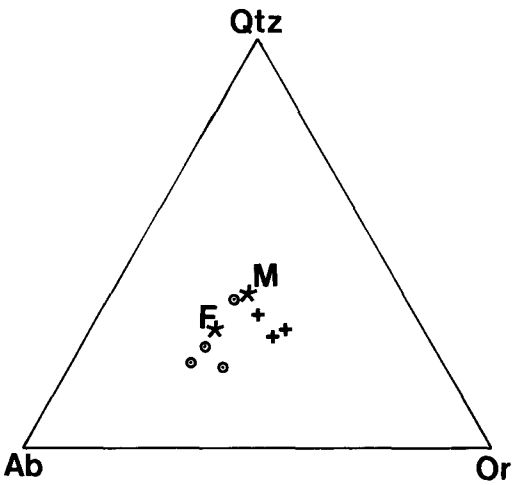

FIG. 4. Modal compositions of silicate melt inclusions and representative whole-rock analyses in the system Qtz–Ab–Or. The point F is the liquidus minimum for this system with excess water and 1% F at 1 kbar pressure (Manning, 1981), M is the minimum for the fluorine-free system (Tuttle and Bowen, 1958). Circles = whole-rock samples; crosses = silicate melt inclusions.

cate melt inclusions are, however, relatively enriched in the Or component. High normative Or/Ab ratios were also found for the granophyric part of the Notch Peak granite, Utah, which probably crystallized from a fluid phase (Nabelek, 1986).

Aegirine and/or alkali amphibole occur both in the miarolitic cavities and as late-crystallized minerals in the rock proper. Furthermore, most feldspars are rimmed by nearly pure albite. We propose that the alkali contents in the late-magmatic silicate melt inclusions reflect the late-magmatic processes: Na (and Fe) was continuously consumed in the formation of alkali pyriboles, and the residual melts therefore became depleted in Na relative to K.

It should be noted that formation of aegirine requires that the magmatic system is peralkaline (i.e. that molecular Na + K > Al) (Bailey, 1969). The ESG residual melts in question are not peralkaline (Table 2). It can therefore be suggested that the coexisting, magmatic fluid phases (liquid + vapour) had alkali to alumina ratios high enough to make the late-magmatic system peralkaline in spite of lacking peralkalinity in the melt inclusions.

Acknowledgements

Field work was supported by the Norwegian Council for Scientific and Technical Research (NTNF) through E.-R. Neumann. Facilities for microprobe analyses were provided by the Free University in Amsterdam and by the WACOM, a working group for analytical chemistry of minerals and rocks; this group is subsidized by the Netherlands Organization for the Advancement of Pure Research (ZWO). H. van Egmond made a beautiful microprobe sample. E.-R. Neumann, T. Andersen, N. Oskarsson and two anonymous reviewers are thanked for helpful suggestions and critical comments. This is Norwegian ILP-contribution no. 98.

References

Andersen, T. (1981) *En geokjemisk-petrologisk undersökelse av de intrusive bergartene i Sande Cauldron, Oslofeltet.* Unpubl. Cand. Real. thesis, Univ. of Oslo.

——(1984) Crystallization history of a Permian composite monzonite–alkali syenite pluton in the Sande cauldron, Oslo rift, southern Norway. *Lithos*, **17**, 153–70.

Bailey, D. K. (1969) The stability of acmite in the presence of H_2O. *Am. J. Sci. Schairer vol.* **267A**, 1–16.

Bailey, J. M. (1977) Fluorine in granitic rocks and melts: a review. *Chem. Geol.* **19**, 1–42.

Barth, T. F. W. (1945) Studies of the igneous rock complex of the Oslo Region. II. Systematic petrography of the plutonic rocks. *Skr. Nor. Vitensk. Akad. Oslo I.* (1944) **3**, 1–104.

Bowen, N. L. (1937) Recent high-temperature research on silicates and its significance in igneous geology. *Am. J. Sci.* **33**, 11–21.

Brøgger, W. C. (1890) Die Mineralen der Syenitpegmatitgange der sud-norwegishen Augit- und Nephelinsyenite. *Zeits. Kryst. Mineral.* **16**, 1–663.

——(1906) Eine sammlung der wichtigsten Typen der Eruptivgesteine des Kristianiagebites. *Nyt Mag. Naturvidensk.* **44**, 115–44.

——and Schetelig, J. (1926) Rektangelkart Kongsberg 1:100 000), *Norges Geol. Unders.*

Burnham, C. W. (1979) Magmas and Hydrothermal Fluids. In *Geochemistry of hydrothermal ore deposits*, 2nd edn. (Barnes, H. L., ed.) J. Wiley & Sons, 71–136.

Chou, I. M. (1987) Phase relations in the system NaCl–KCl–H_2O. III. Solubilities of halite in vapor-saturated liquids above 445 °C and redetermination of phase equilibrium properties in the system NaCl–H_2O to 1000 °C and 1500 bars. *Geochim. Cosmochim. Acta* **51**, 1965–75.

Clynne, M. A. and Potter, R. W. II. (1977) Freezing point depression of synthetic brines (abstr.). *Geol. Soc. Am. Abstr. Programs* **9**, 930.

Dietrich, R. V., Heier, K. S. and Taylor, S. R. (1965) Studies on the igneous rock complex of the Oslo Region. XX. Petrology and geochemistry of ekerite. *Skr. Nor. Vidensk.-Akad. Oslo. I. Ny ser.* **19**, 1–31.

Dingwell, D. B., Harris, D. M. and Scarfe, C. M. (1984) The solubility of H_2O in melts in the system SiO_2–Al_2O_3–Na_2O–K_2O at 1 to 2 kbars. *Journ. Geol.* **92**, 387–95.

Gaut, A. (1981) Field relations and petrography of the biotite granites of the Oslo region. *Norges Geol. Unders.* **367**, 39–64.

Hansteen, T. H. (1988) *Cooling history of the Eikeren–Skrim peralkaline granite complex, the Oslo Region, Norway. Evidence from fluid inclusions and mineralogy.* Unpubl. Cand. Scient. thesis, Min.-Geol. Museum, Univ. of Oslo, 244 pp.

——and Burke, E. A. J. (1989) Melt–mineral–fluid interaction in peralkaline silicic intrusions in the Oslo Rift, Southeast Norway. II. High-temperature fluid inclusions in the Eikeren–Skrim granite complex. *Norges geol. Unders.* 00.00.

Heier, K. S. and Compston, W. (1969) Rb–Sr studies of the plutonic rocks of the Oslo region. *Lithos*, **2**, 133–45.

Holland, H. D. (1972) Granites, solutions and base metal deposits. *Econ. Geol.* **67**, 281–301.

Manning, D. A. C. (1981) The effect of fluorine on liquidus phase relationships in the system Qz–Ab–Or with excess water at 1 kb. *Contrib. Mineral. Petrol.* **76**, 206–15.

——Hamilton, D. L., Henderson, C. M. B. and Dempsey, M. J. (1980) The probable occurrence of interstitial Al in hydrous, F-bearing and F-free aluminosilicate melts. *Contrib. Mineral. Petrol.* **75**, 257–62.

Nabelek, P. I. (1986) Trace-element modelling of the petrogenesis of granophyres and aplites in the Notch Peak granitic stock, Utah. *Am. Mineral.* **71**, 460–71.

Neumann, E.-R. (1974) The distribution of Mn^{2+} and Fe^{2+} between ilmenites and magnetites in igneous rocks. *Am. J. Sci.* **274**, 1074–88.

——(1976) Compositional relations among pyroxenes, amphiboles and other mafic phases in the Oslo Region plutonic rocks. *Lithos*, **9**, 85–109.

——(1978) Petrology of the plutonic rocks. In *The Oslo Paleorift, A Review and Guide to Excursions, Norges Geol. Unders.* **337** (J. A. Dons and B. T. Larsen eds.) 25–34.

——(1980) Petrogenesis of the Oslo Region larvikites and associated rocks. *J. Petrol.* **21**, 498–531.

——Brunfelt, A. O. and Finstad, K. G. (1977) Rare earth elements in some igenous rocks in the Oslo rift, Norway. *Lithos*, **10**, 311–9.

——Tilton, G. R. and Tuen, E. (1988) Sr, Nd and Pb isotope geochemistry of the Oslo rift igenous province, southeast Norway. *Geochim. Cosmochim. Acta*, **52**, 1997–2008.

——Andersen, T. and Hansteen, T. H. (1989) Melt-mineral-fluid interaction in peralkaline silicic intrusions in the Oslo Rift, Southeast Norway. I. Geochemistry of the Eikeren ekerite. *Norges Geol. Unders.* 00.00.

Nystuen, J. P. (1975) Plutonic and subvolcanic intrusions in the Hurdal area, Oslo region. *Norges Geol. Unders.* **317**, 1–21.

Oftedahl, C. (1978) Origin of the lavas of the Vestfold lava plateu. In *Petrology and geochemistry of Continental Rifts. NATO ASI series C*, **36** (E.-R. Neumann and I. B. Ramberg, eds.) D. Reidel, 193–208.

Poty, B., Leroy, J. and Jachimowicz, L. (1976) Un nouvel appareil pour la mesure des temperatures sous le microscope: 1 installation de microthermometrie Chaixmeca. *Bull. Soc. Fr. Mineral. Cristallogr.* **99**, 182–6.

Raade, G. (1972) Mineralogy of the miarolitic cavities in the Plutonic Rocks of the Oslo Region, Norway. *Mineral. Record* **3**, 7–11.

——(1973) *Distribution of radioactive elements in the plutonic rocks of the Oslo Region.* Unpubl. Cand. Real. thesis, Univ. of Oslo, 162 pp.

——(1978) Distribution of Th, U, K in the plutonic rocks of the Oslo Region, Norway. In *Petrology and geochemistry of continental rifts. NATO ASI series C*, **136** (E.-R. Neumann and I. B. Ramberg, eds.) D. Reidel. 185–92.

Ramberg, I. B. (1976) Gravity interpretation of the Oslo Graben and associated igneous rocks. *Norges Geol Unders.* **325.**

——and Larsen, B. T. (1978) Tectonomagmatic evolution. In *The Oslo Paleorift, A Review and Guide to Excursions, Norges Geol. Unders.* **337** (J. A. Dons and B. T. Larsen, eds.) 55–73.

Rasmussen, E., Neumann, E.-R., Andersen, T., Sundvoll, B., Fjerdingstad, V. and Stabel, A. (1988) Petrogenetic processes associated with intermediate and silicic magmatism in the Oslo rift, south-east Norway. *Mineral. Mag.* **52**, 293–307.

Roedder, E. (1984) *Fluid inclusions. Reviews in Mineralogy*, **12**, 644 pp.

——and Coombs, D. S. (1967) Immiscibility in granitic melts, indicated by fluid inclusions in ejected granitic blocks from Ascencion Island. *J. Petrol.* **8**, 417–51.

Sæther, E. (1962) Studies on the igneous rock complex of the Oslo region, XVIII. General investigations of the igneous rocks in the area north of Oslo. *Skr. Nor. Vidensk. Akad. Oslo I. Ny ser.* **1**, 184 pp.

Sterner, S. M., Hall, D. L. and Bodnar, R. J. (1988) Synthetic fluid inclusions. V. Solubility relations in the system NaCl–KCl–H_2O under vapour-saturated conditions. *Geochim. Cosmochim. Acta*, **52**, 989–1005.

Sundvoll, B. (1978) Rb/Sr-relationship in the Oslo igneous rocks. In *Petrology and geochemistry of conti-*

nental rifts. NATO ASI series C, **136** (E.-R. Neumann and I. B. Ramberg, eds.) D. Reidel. 181–4.

Thompson, R. N. and MacKenzie, W. S. (1967) Feldspar–liquid equilibria in peralkaline acid liquids: An experimental study. *Am. J. Sci.* **265**, 714–34.

Tuttle, O. F. and Bowen, N. L. (1958) Origin of granite in the light of experimental studies in the system $NaAlSi_3O_8$–$KAlSi_3O_8$–SiO_2–H_2O. *Geol. Soc. Am. Mem.* **74**, 153 pp.

Weast, R. C. (1984) *Handbook of chemistry and physics*. CRC press, Cleveland, Ohio.

[*Manuscript received 4 July 1989; revised 6 December 1989*]